CrossMark
click for updates

Injection deep level transient spectroscopy: An improved method for measuring capture rates of hot carriers in semiconductors

R. M. Fleming, C. H. Seager, D. V. Lang, and J. M. Campbell
Sandia National Laboratories, Albuquerque, New Mexico 87185-1415, USA

An improved method for measuring the cross sections for carrier trapping at defects in semiconductors is described. This method, a variation of deep level transient spectroscopy (DLTS) used with bipolar transistors, is applied to hot carrier trapping at vacancy-oxygen, carbon-oxygen, and three charge states of divacancy centers (V_2) in n- and p-type silicon. Unlike standard DLTS, we fill traps by injecting carriers into the depletion region of a bipolar transistor diode using a pulse of forward bias current applied to the adjacent diode. We show that this technique is capable of accurately measuring a wide range of capture cross sections at varying electric fields due to the control of the carrier density it provides. Because this technique can be applied to a variety of carrier energy distributions, it should be valuable in modeling the effect of radiation-induced generation-recombination currents in bipolar devices. © *2015 AIP Publishing LLC*.
[http://dx.doi.org/10.1063/1.4923358]

I. INTRODUCTION

Predicting changes in semiconductor device currents due to radiation-induced traps typically begins with an investigation of Shockley-Read-Hall (SRH) recombination currents[1–3] that are induced by the traps. A calculation of SRH recombination rates requires knowledge of all parameters of the trap. This includes the trap energy level, plus the rates of emission and capture of both electrons and holes. Trap energy levels and carrier emission rates can be readily measured as a function of electric field strength using deep level transient spectroscopy (DLTS).[4–6] Capture rates are more difficult to measure and are the focus of this study. For electrons with carrier density n, moving with average velocity v, the electron capture rate c_n is related to electron capture cross section σ_n by

$$c_n = \sigma_n \langle v \rangle n. \qquad (1)$$

A similar equation exists for hole capture rates, cross sections, and densities. It is important to remember that capture cross sections can be quite sensitive to both the electric field and to the energy distribution of the carriers,[7–9] and that this dependence requires specifying the location of the recombination process in the device of interest. Many devices, bipolar transistors being a good example, have radiation-induced gain losses which are primarily due to generation-recombination currents in emitter-base space charge regions. In these high field environments, carriers typically have effective temperatures much higher than the lattice temperature, and capture rates can be different from those for thermal carriers. By contrast, recombination of injected carriers with majority carriers in the neutral base of these devices is properly modeled with capture rates measured under thermal equilibrium conditions.

Experiments to measure carrier capture face several experimental difficulties. Typical DLTS-based measurements involve reducing the bias on reverse-biased diodes for short

periods of time to allow traps to refill with majority carriers in thermal equilibrium. Because available diodes usually have majority carrier densities well in excess of $10^{14} \, \mathrm{cm}^{-3}$, capture rates can be quite high. Measurements of capture rates in these diodes require short filling pulses, which can be difficult to experimentally implement. An indirect method of estimating capture cross sections that has sometimes been employed involves determining the prefactor of an Arrhenius plot of the emission rate versus the inverse temperature.[5] The equation used for this estimate is based on three assumptions: (1) The capture rate which is calculated is that appropriate for the electric field conditions where emission was measured, (2) the carriers captured by the traps are in thermal equilibrium with the lattice, and (3) there is no thermal barrier to capture. As a further complication, the cross section, which is part of the prefactor, requires the data to be extrapolated to zero inverse temperature. The Arrhenius plot is theoretically based on the thermodynamic free energy, but the experimental data are based on the enthalpy.[5,6,10] As is well known, care should be taken in using Arrhenius emission rate plots to extract capture cross sections, particularly for deep, non-hydrogenic levels and for levels where the emission rate is affected by electric fields.[5,6,11] Given these difficulties, there is clearly a need for improved experimental methods which measure capture rates at a variety of electric fields and carrier energy distributions.

In this paper, we describe a method for filling traps that can be used for measuring capture rates when the DLTS diode is part of a bipolar transistor. We call this technique injection-DLTS (inj-DLTS). In inj-DLTS, the measured diode is held at constant reverse bias, while the carriers used to fill the traps originate from a forward-bias pulse of the adjacent diode of the bipolar transistor. For example, if one uses inj-DLTS to measure traps in the collector of a bipolar transistor, traps are filled by pulsing the base-emitter diode into forward bias while holding the measured diode at a constant reverse bias. This injects minority carriers into the

118, 015703-1

base, which results in a pulse of majority carriers in the collector. There are two primary ways that this method of trap filling differs from standard DLTS (1) carriers are captured from a population that is not in thermal equilibrium and (2) the capture rate can be controlled by varying the current in the forward-bias pulse of the emitter-base junction. Thus instead of a fixed, fast capture rate set by the diode doping, a variable capture rate is provided by control of the emitter-base current pulse. With a slower capture rate, the roll-off of the DLTS emission signal versus filling pulse width moves to longer times that are more accessible experimentally.

In addition to the advantages for measuring capture cross sections, inj-DLTS also offers advantages in measurements of trap emission rates. In standard DLTS traps within the zero-bias depletion zone set by the built-in voltage of the diode are not filled, hence these traps near the metallurgical junctions are not part of the DLTS spectrum. This is not the case with inj-DLTS since trap filling occurs over the entire depletion zone. Another advantage is the ability to inject minority carriers into a diode without the presence of majority carriers. In standard minority carrier DLTS, traps are filled with minority carriers by short pulses of the measured diode into forward bias. During trap filling, traps are simultaneously exposed to both minority and majority carriers. When implementing inj-DLTS using the reverse biased emitter-base diode of a transistor as the measured diode, one can capture minority carriers by forward biasing the adjacent base-collector junction. In this case, there is a pulse of minority carriers into the emitter/base depletion region with no competing capture of majority carriers. This is an advantage shared with optical filling techniques.[12] When combined with standard majority carrier DLTS, inj-DLTS offers the ability to see DLTS signals from traps that span the entire band gap.

II. THEORY

Before discussing experimental results from this technique, it is important to consider how carriers injected into depleted regions of reversed biased p/n junctions are transported. To explore this, we write the standard drift/diffusion equations for transport of injected electrons and consider the motion of charge in an (abrupt) depletion zone with constant doping and negligible carrier recombination. For inj-DLTS using injection from the emitter-base junction and measurements of the collector (forward active mode of the transistor), the assumption of negligible recombination is well satisfied for the samples discussed here. Forward active Gummel measurements show little difference between the emitter current and the collector current both before and after the introduction of radiation defects. Measurements of minority carrier inj-DLTS using the transistor base and injection from the base-collector junction (reverse active mode) will be discussed separately below. The injected current can be written as

$$J = q[n(x)\mu(x)\mathcal{E}(x) + D(x) \cdot dn(x)/dx]. \quad (2)$$

Here q the electronic charge, $n(x)$ is the electron concentration, $\mu(x)$ the electron mobility, $\mathcal{E}(x)$ the electric field, and $D(x)$ the electron diffusivity all measured at the local position, x. It has been shown that $D(x)$ can be related to $\mu(x)$ by the Einstein relation even in the absence of thermal equilibrium.[13,14] In the experiments of interest for this paper capture rates of electrons at traps are proportional to the local value of $n(x)$, so we are interested in exploring the detailed spatial dependence of this density.

There is no analytic solution to Eq. (2), even for constant carrier mobility and a linear spatial dependence of the electric field. In our experiments $\mu(x)$ varies over our depleted regions because of the high electric fields, and only numerical methods are useful in calculating the spatial dependence of $n(x)$. To address this problem numerically we replace the derivative in Eq. (2) with differences, divide our depleted regions into small spatial slices and iterate the dependence of $n(x)$, starting at the known values of majority carrier density and injected current at the edge of the (collector) depleted region. The experimentally established relationship between $\mu(x)$ and $\mathcal{E}(x)$ for electrons in Si was used in this calculation.[15,16] The self-consistent values of $n(x)$ calculated for two widely different values of J are shown in Fig. 1 for conditions appropriate to our npn base/collector diode biased at -5 V at 128 K. Note that $n(x)$ is nearly constant over the entire depletion zone except for a region near the diode depletion edge where the tail of the majority carriers from the neutral region is evident. The difference curve of the two currents, shown as the solid line, illustrates that the injected carrier density is also constant even for most of the tail region near the depletion edge. The spatially uniform charge density can be anticipated. First, we assume that J is conserved and we can show the carrier velocity, which is the product of $\mu(x)$ and $\mathcal{E}(x)$ is saturated over most of the electric field range in this calculation (and also at the electric fields of our experimental data).[15] In addition diffusion current is negligible over most of the depleted region at these low carrier densities. Consequently, dominance of the first term in Eq. (2) leads to a density of carriers that is nearly spatially independent. In the region near the depletion edge,
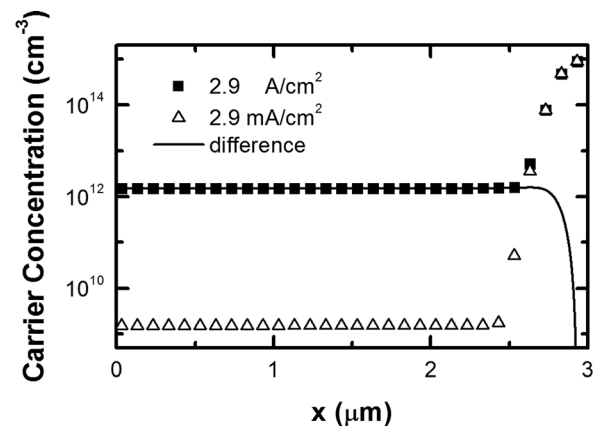

FIG. 1. Calculated carrier concentration versus distance from the metallurgical junction of a base/collector diode for two different injected current densities, 2.9 A/cm^2 (closed squares) and 2.9 mA/cm^2 (open triangles). The difference between the two densities is also shown as a solid line. The difference density is responsible for the transient response of the diode capacitance to the pulse of injected carriers and is equal to the large current density over nearly all of the depleted diode.

the injected carrier density becomes very small and is of no consequence in our inj-DLTS measurements. Traps in this region are below the Fermi level and are filled before injection. Hence they do not contribute to our observed emission transients. These simulations show that, for field independent capture, capture rates during carrier injection are expected to be almost independent of depth, a result that greatly simplifies interpretation of transient capacitance data.

III. EXPERIMENTAL DETAILS

We have measured DLTS from electron damaged npn (2N2222) and pnp (2N2907) silicon bipolar junction (BJT) transistors. All transistors received the same level of damage in a single run using 25 MeV electrons at a Linac at the Little Mountain Test Facility (Hill AFB, UT). The approximate dose was 25 Mrad (Si) ($\sim 5.8 \times 10^{14} \, cm^{-2}$) for transistors used for inj-DLTS in the collector and about 130 Mrad for one transistor used for minority carrier inj-DLTS in the base. The doping levels of these transistor diodes were determined by SIMS, spreading resistance and CV measurements. The doping levels are similar for both the npn and pnp devices with base doping of about $3 \times 10^{16} \, cm^{-3}$ and collector doping of $9 \times 10^{14} \, cm^{-3}$ for the npn and $2 \times 10^{15} \, cm^{-3}$ for the pnp. The dopants are P for n-type and B for p-type silicon.

A bipolar transistor consists of two back-to-back diodes, an emitter-base diode and a base-collector diode. Typically the emitter diode is highly doped ($\sim 10^{18} \, cm^{-3}$), the base is intermediate doped ($\sim 10^{16} \, cm^{-3}$), and the collector is low-doped ($\sim 10^{15} \, cm^{-3}$). In normal forward-active transistor operation, the emitter-base diode is forward biased resulting in a flow of injected carriers from the emitter to the reverse-biased collector.

We have performed capacitance based DLTS measurements using a Boonton 7200 1-MHz bridge on both of the transistor diodes. We measure defects in the collector by reverse biasing the base-collector junction and defects in the base by reverse biasing the emitter-base junction. In the standard DLTS method, traps are filled by repetitively pulsing the reverse biased junction to a smaller bias, typically zero volts. During the filling pulse traps are filled with the large density of majority carriers present in the part of the device containing the depletion region (collector or base). With inj-DLTS traps are filled using a pulse of current from the second transistor diode. For the case of DLTS in the collector, the base-collector junction is held at a fixed reverse bias, while the emitter-base diode is pulsed into forward bias. This results in a minority carrier pulse in the base that transits to the collector where it becomes a majority carrier pulse. For the case of DLTS in the base, the emitter-base junction is held at fixed reverse bias and a forward-bias pulse of the base-collector junction results in a minority carrier pulse in the base. In transistor parlance, this second configuration is referred to as the reverse active mode. In both cases, traps are filled with a carrier density that is controlled by the amplitude of the forward-bias current pulse. The effective temperature of the injected hot carriers is controlled by the magnitude of the reverse bias on the measured diode.

For standard DLTS measurements, the filling pulse was applied either through the Boonton external bias input (wide pulses) or via a pulse transformer on the low side of the Boonton input (narrow pulses). The wide pulse configuration with the bias controlled via the Boonton external bias input could be used for filling pulses from 30 μs to 1 s. The minimum pulse width is set by the capacitance bridge circuitry. Narrower filling pulses could be employed by using an external pulse transformer driven by an external voltage source and located on the low side of the Boonton sample input.[17] In the transformer configuration, the external bias input of the Boonton is held at a constant reverse bias and a positive pulse is applied via the pulse transformer. The pulse transformer configuration allows shorter filling pulses in the range of 200 ns–100 μs. The 200 ns lower limit of the pulse width is imposed by the minimum rise time that can be achieved with the Boonton capacitance bridge in the circuit. This technique can be used to measure equilibrium capture rates; however, the 200 ns minimum pulse limit is marginal for optimum measurements using diodes with doping of order $10^{15} \, cm^{-3}$. This means the largest cross section we can measure is about $5 \times 10^{-16} \, cm^2$. As a result we are unable to fully cover the entire range of trap occupation using standard DLTS; however, as we shall show below, this is not a limitation for the inj-DLTS technique.

With majority carrier inj-DLTS, the measured diode is held at constant bias, while the second diode of the BJT is pulsed into forward bias via an external voltage source. In this configuration pulse widths of 20 μs–1 s can be applied. Again, the minimum pulse width is controlled by the rise time of the circuit with the capacitance bridge. Pulses were monitored by a fast oscilloscope and in all cases the rise time of the pulse is negligible relative to pulse width, resulting in a rectangular current pulse. The forward bias current was controlled with one of five calibrated current limiting diodes in the range of 30 μA–1 mA; these were inserted in series with the external pulse source. The injected current controls the carrier density in the reverse biased base/collector diode and therefore the capture rate. The use of these diodes in the inj-DLTS configuration allows conventional temperature scans to be made with a constant density of carriers analogous to standard DLTS measurements.

Minority carrier inj-DLTS was employed in the base of an npn transistor using minority carriers injected from forward biasing the base-collector junction. This technique differs from standard minority carrier DLTS where traps are filled by pulsing the measured diode into forward bias. With minority carrier inj-DLTS traps are filled only with minority carriers and there is no competing capture from majority carriers. Care must be taken in determining the injected carrier density, however. Unlike inj-DLTS in the collector where the injected carriers arise from pulsing the transistor into forward active mode, this configuration pulses the transistor into reverse active mode. Because these samples are more heavily damaged than those used for majority carrier inj-DLTS, considerable recombination occurs in the neutral base before the carriers reach the emitter-base depletion region. This can be quantified by making reverse Gummel measurements at the same temperature as the emission measurement.

Rather than using the value of the current limiting diode to measure the injected current, the smaller value of the emitter current obtained from the reverse Gummel is used.

IV. EXPERIMENTAL RESULTS

Figure 2(a) shows standard and inj-DLTS temperature scans of the collector of an electron damaged npn transistor measured at −5 V bias and a DLTS emission rate of 116/s. The open symbols are data using conventional trap filling where the collector is pulsed to 0 V for 100 μs. The closed symbols are injection DLTS where the collector is held at a constant −5 V bias and the emitter-base junction is pulsed into forward bias (350 μA for 2.8 ms). The injected current density is approximately 1 A/cm^2. In Fig. 2(a), the magnitudes of C for the inj-DLTS data have been reduced by a factor of 1/2.5 to overlay the plots of $\Delta C/C$. The 1/2.5 reduction is consistent with the smaller area of the emitter contacts as compared with the area of the collector on these transistors. The diagram in Fig. 2(a) is a top view of a typical BJT showing that the area of the emitter-base junction is smaller than the area of the base-collector junction. This implies that only
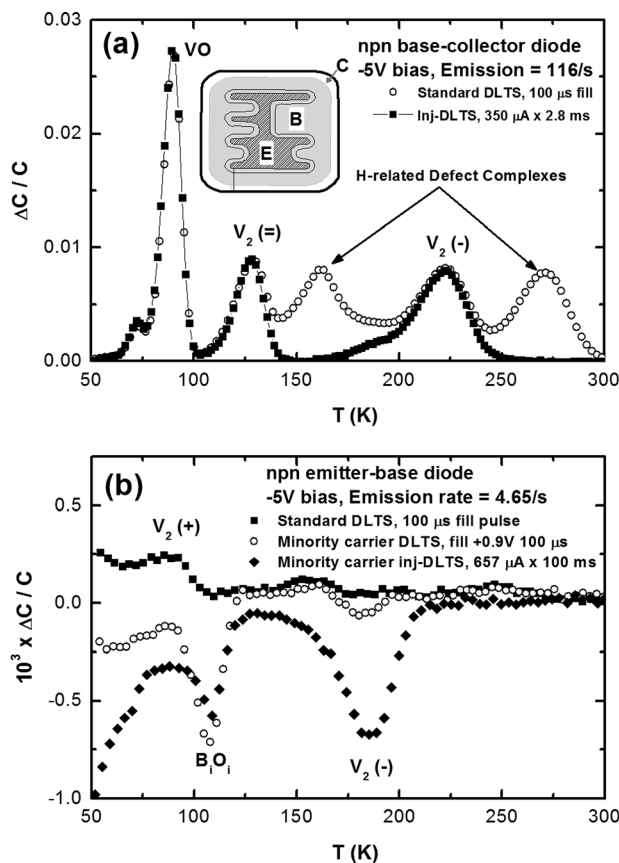

FIG. 2. (a) DLTS of the collector junction of an electron damaged npn BJT at −5 V bias obtained by standard trap filling at 0 V and by inj-DLTS from the emitter-base. Standard trap filling produces two additional peaks that we assign to hydrogen related defect complexes. The H-related complexes are located near the periphery of the collector and these traps are not filled when using inj-DLTS. The diagram is a plan view of a typical BJT illustrating that the area of the emitter-base diode is both smaller than the base-collector diode cross section and contained within it. (b) DLTS of the base junction of an electron damaged npn BJT at −5 V bias obtained by standard trap filling, by standard minority carrier DLTS, and by minority carrier inj-DLTS from the base-collector junction.

traps under the emitter contacts are filled when using inj-DLTS, a notion that is also supported by the two additional DLTS peaks seen in the standard DLTS scan (open symbols). These extra peaks are seen after electron damage of silicon BJT's, but not after heavy ion or neutron damage. The extra peaks may be due to H-related defect complexes.[12,18,19] Ionizing radiation is known to cause passivating hydrogen to be released from the oxides.[20] The released hydrogen diffuses to the periphery of the transistor where it encounters and reacts with displacement defects. The H-related peaks are not seen in inj-DLTS since the H-related defects are not located under the emitter electrode. Hence they do not fill after the pulse of injected current.

Figure 2(b) shows the results from the base of a second npn transistor with about five times more damage. Three spectra are shown. Standard majority carrier DLTS of the base diode with 0 V filling and an emission rate of 4.65/s that shows p-type DLTS peaks is plotted with closed squares. Traditional minority carrier DLTS where the filling is at +0.9 V is plotted as open circles. A spectrum of inj-DLTS obtained by a forward bias pulse of the base-collector junction is plotted as closed diamonds. Note that the peak labeled B$_i$O$_i$ is about the same size in both minority carrier DLTS and inj-DLTS. In minority carrier DLTS B$_i$O$_i$ has been shown to be dominant over V$_2$(=) (which appears at about the same temperature in majority carrier n-type DLTS) because V$_2$(=) has a very large hole capture cross section.[21,22] We retain the same peak identification in inj-DLTS. In contrast V$_2$(-) is much larger in the inj-DLTS spectrum than it is in the minority carrier DLTS spectrum due to the absence of competing capture by holes.

For a given trap and capture cross section, the capture rate is described by Eq. (1) and is proportional to the carrier density and the average carrier velocity. For standard DLTS with filling at equilibrium, the capture rate is fixed at a value determined by the equilibrium carrier density and the average thermal velocity. For a Maxwellian velocity distribution, the mean thermal velocity is $v_{th} = \sqrt{8kT/\pi m^*}$ where m^* is the effective mass of the carrier. We use averaged silicon density of states electron mass of $m_e^* = 0.33\,m_e$ and the heavy hole mass of $m_h^* = 0.49\,m_e$. This formula results from a proper averaging of the carrier velocity in a parabolic band. In the measurements described here carrier motion is severely perturbed by the large electric fields in the junction depletion regions; electrons are primarily moving parallel to the electric field gradient, and the carrier drift velocity is saturated. Under these conditions, we believe that the appropriate velocity to use in Eq. (1) is the saturated drift velocity v_{sat}. We note that over the temperature region of these measurements v_{sat} and v_{th} differ by no more than 50%. The product of the saturated drift velocity and the carrier density used in Eq. (1) can be obtained from the injected current density, $v_{sat}n = J/q$ where q is the electronic charge. For the case of minority carrier inj-DLTS (reverse bias emitter-base junction, forward bias base-collector junction), the correct current density is the emitter current obtained from a reverse-Gummel measurement, not the injected current from the current limiting diode (J_c).

For inj-DLTS, the saturated carrier drift velocity is used in Eq. (1), but more importantly the carrier density is controlled by the amplitude of the forward-bias current pulse. This allows control of the capture rate and access to capture rates that would be too fast to measure in neutral material. The amplitude of the DLTS transient ΔC as a function of the filling pulse width is given by[6]

$$\Delta C(t_f) = \Delta C_{max} \left[\frac{c}{(c+e)} \right] * \left[1 - \exp(-t_f(c+e)) \right], \quad (3)$$

where ΔC_{max} is the amplitude of the capacitance transient when all traps are filled, c is the capture rate, e is the emission rate, and t_f is the width of the filling pulse. This equation is obtained from a solution of the general rate equation for trap occupancy. There are two adjustable parameters, ΔC_{max} and c with the emission rate, e, fixed at a value determined by the temperature.

An example of the measurements of DLTS versus the injection pulse width is shown in Fig. 3(a) where we plot measurements of $\Delta C/C$ using the divacancy acceptor $V_2(+)$ in the collector of a pnp transistor as a function of the log of
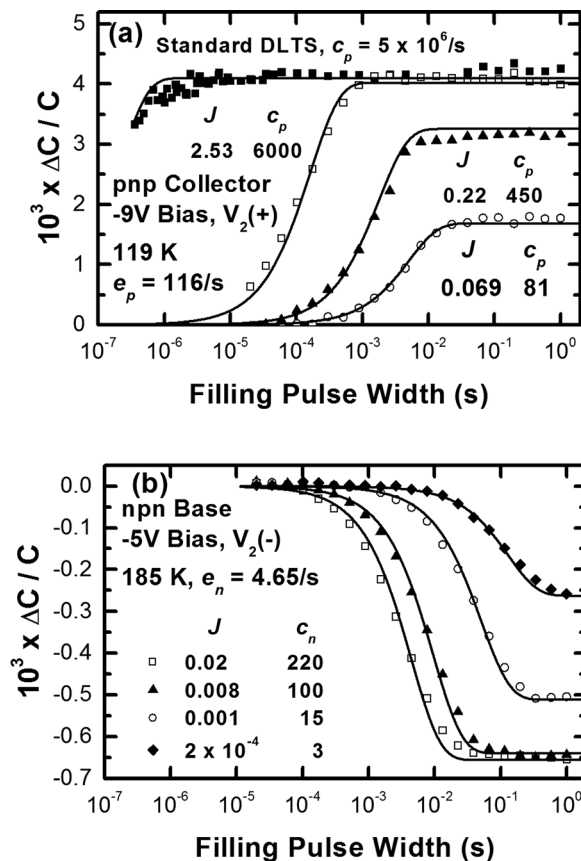

FIG. 3. (a) DLTS of a silicon pnp BJT at 119 K (divacancy donor $V_2(+)$ at -9 V) as a function of the trap filling pulse width. Standard-DLTS capture using 0 V filling (solid squares) and injection-DLTS at three levels of injected current are shown. The lines are fits to Eq. (3) with hole capture rates, c_p, shown. For the three injection-DLTS examples, injection current densities in units of A/cm² and capture rates in units of s⁻¹ are indicated. (b) Minority carrier inj-DLTS of a silicon npn BJT at 185 K (divacancy single acceptor $V_2(-)$ at -5 V) as a function of the trap filling pulse width. The lines are fits to Eq. (3). Values of the injection current densities in units of A/cm² and capture rates in units of s⁻¹ are indicated.

the filling pulse width. The data were taken using a bias of -9 V at 119 K and a DLTS emission rate of $e = 116$/s. We show data for both standard DLTS with 0 V filling (solid squares) and data for three current levels of inj-DLTS. As can be seen, the standard DLTS filling technique is only marginally adequate in determining the thermal, low field capture rate. In all data, the lines are fits of Eq. (3) to the data with values of the hole capture rate c_p in units of s⁻¹. For the three examples of inj-DLTS, the current densities J in units of A/cm² are also indicated. Note that for the temperature and emission rate chosen, the traps are only about half filled at the smallest value of injected current and this behavior is captured by fits to Eq. (3). This result is a consequence of the emission (e) and capture (c_p) rates being nearly equal.

An example of capture data obtained from minority carrier inj-DLTS is shown in Fig. 3(b) where we show capture into the $V_2(-)$ defect at -5 V. Emission is from the $V_2(-)$ level located in the p-type base of an npn transistor. Traps are filled by minority carriers obtained by pulsing the base-collector junction into forward bias. In order to obtain sufficient signal, this sample had about five times the dose of the devices used for majority carrier inj-DLTS. Note that the capture rates and the injected current densities are significantly smaller than the majority carrier inj-DLTS shown in Fig. 3(a). This is because, unlike the majority carrier inj-DLTS example, most of the carriers injected into the forward biased base-collector junction recombine before reaching the emitter-base junction. With majority carrier inj-DLTS, we used the value of the current limiting diode to determine J. For minority carrier inj-DLTS, the actual current density in the emitter-base junction during the pulse was determined from a reverse-Gummel measurement at the measurement temperature, here 185 K. For minority carrier inj-DLTS, we only measured capture at $V_2(-)$. We do not report capture at B_iO_i because capture curves at that defect were stretched out making determination of a unique capture rate difficult. This may be due to competition from $V_2 (=)$ which occurs near the same temperature.

Figure 4 show plots of the capture rates from the fits to the inj-DLTS data presented in Fig. 3 as a function of $J/q = v_{sat}n, p$. The capture cross sections for inj-DLTS can be obtained from the slope of the plots. For the case of minority carrier inj-DLTS (Fig. 4(b)), the current used to calculate v_sn is taken from a reverse Gummel plot at 185 K rather than the value of the current limiting diode. These type of plots were used to deduce capture cross sections for five electron induced damage peaks in silicon BJT's. For n-type silicon, these include the vacancy oxygen (VO) and the two divacancy acceptor states $V_2(-)$ and $V_2(=)$. For p-type silicon, we measured capture cross sections of the divacancy donor transition, $V_2(+)$, and the carbon oxygen center (CO). A variety of base/collector depletion biases were employed during this study because we observed that capture rates were sometimes dependent on the electric field strength. An example of this dependence is shown in Fig. 5 for electron capture at the VO center. In Fig. 5, we show the variation in the capture curves for four values of bias. As the bias is increased the capture rate decreases as evidenced by the shift of the capture curve to longer pulse widths. This dependence
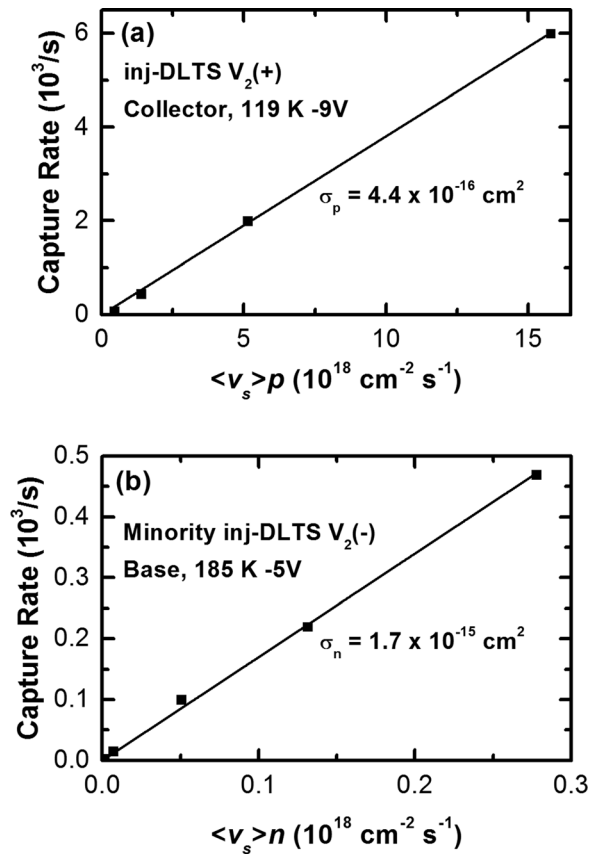
FIG. 4. Capture rates versus the product of the injected carrier concentration and the saturated drift velocity obtained from $J/q = v_{sat}n$: (a) $V_2(+)$ at 119 K and -9 V and (b) minority carrier inj-DLTS $V_2(-)$ at -5 V.

is rather weak but is well outside experimental error and is typical for all three electron trap transitions. The insert to Fig. 5 shows the measured capture rate as a function of the average electric field. Data are fit by a power law of the average field. By contrast, data from the two hole traps showed very little electric field dependence.

For two defects that have small capture cross sections we also measured thermal capture at equilibrium using
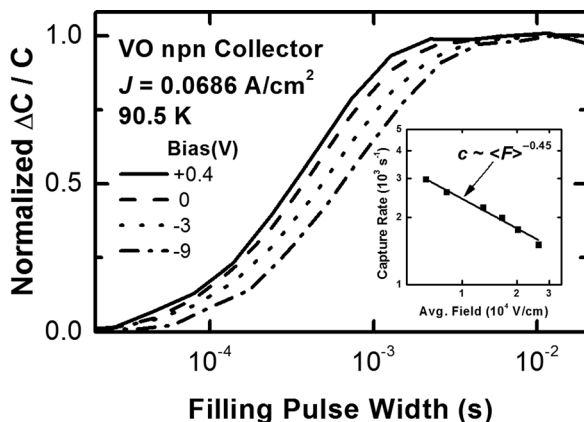

FIG. 5. Normalized inj-DLTS signal as a function of filling pulse width using the smallest value of current injection (lowest capture rate) for four different depletion biases. As the measurement bias is decreased, the capture rate increases. The inset shows a power law fit to the capture rate versus average electric field. A field dependence of the capture rate was seen for each of the electron traps but was not observed for the two hole traps.

standard DLTS at a 0 V filling pulse. An example is shown in Fig. 3(a) showing that the thermal capture data have more uncertainty due to the incomplete capture curve. Cross sections for thermal capture were calculated from the observed capture rates, the diode doping density and the thermal velocity at the temperature of the measurement. Typical capture data in thermal equilibrium and at representative electric fields are shown in Table I.

V. DISCUSSION

The data in Table I indicate some field dependence of the capture rates; hence it is important to consider whether or not the shape of the capture rate curves are affected by the local electric field as the electric field varies significantly across the depletion region. In the case of emission, this question can be easily answered. The electric field dependence of emission rates can be accurately assessed by analyzing the differences between transient capacitance signals at multiple depletion biases, a technique known as double-DLTS (DDLTS).[23] Unfortunately, there is no method for experimentally isolating the analogous effects of the electric field on capture with inj-DLTS. Instead, we will use a self-consistency argument to explore this issue. We start by assuming that the inj-DLTS capture curves closely resemble those expected from carriers captured at the average electric field. To test this hypothesis, we construct and compare two capture rate curves. One curve is obtained by constructing a capture rate curve from Eq. (3) using a single average electric field (no field broadening). The second method constructs a capture rate curve by summing contributions from a series of slices of the depletion region. Each slice has a different electric field and a different capture rate. Figure 5 shows measured capture rate curves for several values of bias taken from the VO peak in the npn collector and a fixed, small value of injection current. We see from the insert of Fig. 5 that the capture rates are well fit by a power law of the average field. We use this power law fit to estimate a capture rate from each slice of the depletion region. We then estimate the amplitude of the DLTS signal of each slice of the depletion region using a well-known linear weighting function sometimes called the "lever rule."[5] The DLTS weighting function is zero at the outer region of the depletion zone where the trap energy is below the Fermi energy, the so-called "dead zone." It then jumps to a maximum value and then linearly decreases to zero at the metallurgical junction.

The results are plotted in Fig. 6 where the line is the prediction of Eq. (3) using a single average capture rate. The symbols are obtained by calculating by weighting the DLTS signal from each slice of the depletion zone, each with a different value of the capture rate obtained from the power law fit. It is clear from Fig. 6 that the spread in capture rates from all parts of the depleted region does not noticeably change the shape of the capture curve from that expected from a single capture rate. In addition, Fig. 6 illustrates that fitting the experimental data with Eq. (3) yields a capture rate which close to that characteristic of the average depletion field. This simulation justifies our starting hypothesis and provides

TABLE I. Carrier capture cross sections for five majority carrier deep levels in silicon. For the $V_2(=)$ and $V_2(+)$ defects thermal capture was measured with standard DLTS, where the diode depletion bias is pulsed momentarily to zero. Capture at non-zero electric fields was measured with inj-DLTS, where carriers were injected into a fixed bias depletion region by forward biasing the emitter-base diode in npn or pnp transistor structures. Data from experiments at three different depletion biases are shown in the last three columns. The maximum electric fields for data in these last three columns are $\mathcal{E}_1 = 1.8 \times 10^4$ V/cm, $\mathcal{E}_2 = 2.9 \times 10^4$ V/cm, and $\mathcal{E}_3 = 5.7 \times 10^4$ V/cm..

Trap	type	E_T (eV)	T (K) e = 116/s	σ_{thermal} (10^{-16}cm^2)	$\sigma_{\mathcal{E}_1}$ (10^{-16}cm^2)	$\sigma_{\mathcal{E}_2}$ (10^{-16}cm^2)	$\sigma_{\mathcal{E}_3}$ (10^{-16}cm^2)
VO	n	0.17	90.5		38.2	27.8	22.9
$V_2(=)$	n	0.23	128.5	1.8	25.1	18.6	12.0
$V_2(-)$	n	0.42	222.8		52.9	46.9	34.9
$V_2(+)$	p	0.20	118.5	1.87	4.25	4.49	4.41
CO	p	0.35	195.5			3.64	3.13

an explanation of why our electron inj-DLTS data closely mimics that expected for a single capture rate.

It is known that there are several competing effects that could make capture processes dependent on electric field.[8] For traps where capture is inhibited due to a repulsive Coloumb potential, electric fields can aid capture due to tunneling of carriers through narrower parts of the Coulomb barrier. For any trap where capture is accompanied by emission of several phonons, the probability of this process declines as the number of phonons increases. The resulting field-induced heating of the electron population will reduce the capture rate. For repulsive centers, these two effects can combine to produce a capture rate which has a non-monotonic dependence on the electric field. In Fig. 7, we plot all of our observed capture cross sections versus the average electric field. In this plot, we have included thermal capture cross section values listed in the literature.[22,24–26] We have also added trend lines representing the general behavior expected for capture at neutral and repulsive traps.[8] The monotonic, downward trend expected for capture at neutral traps is generally consistent with the VO(-) and $V_2(-)$ data. The sharp rise expected at low fields for repulsive center capture is also consistent with prior thermal measurements and our inj-DLTS data for the $V_2(=)$ transition.

In closing we note that over the range of electric fields covered in our capture data we do not observe any noticeable shift of the emission rate of any of the defect transitions we have measured; this further emphasizes the fact that the changes we see in capture are a consequence of the physics of the multi-phonon emission/capture processes and not due to electric field-induced distortions of the defect configurations.

VI. CONCLUSIONS

We have shown that measuring the carrier capture rates of defects under a variety of electric field conditions can be conveniently accomplished by using carrier injection from an adjacent diode in a bipolar transistor structure. By altering the injection bias and pulse widths a wide range of carrier capture cross sections can be accurately measured over a substantial range of fields. Using this technique, we have measured capture of both electrons and holes for several common defects introduced by high-energy electron bombardment of silicon. Plotting these data versus average electric field reveals behavior which is quite different for capture by neutral and repulsive traps. This behavior is qualitatively consistent with prior theoretical models of capture at high electric fields.
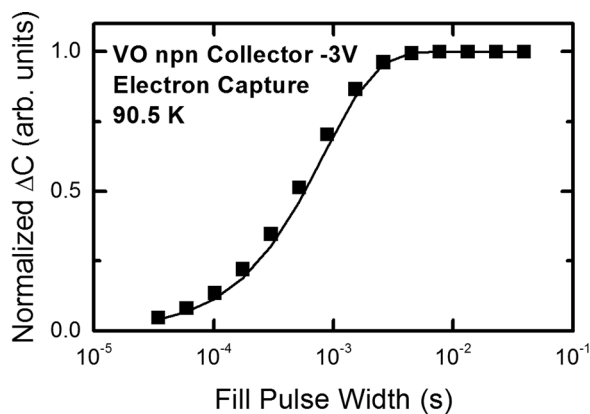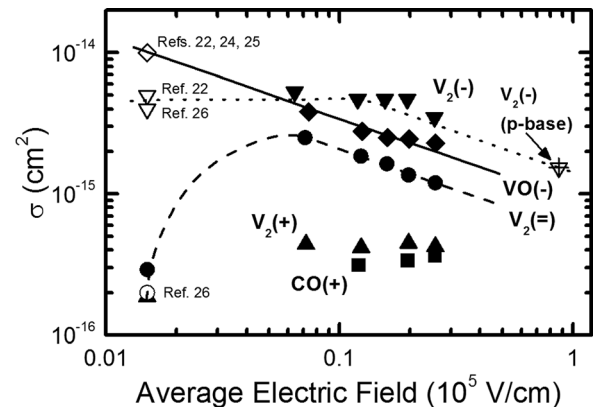

FIG. 6. A comparison of a capture rate curve obtained for the VO defect using Eq. (3) and a single capture rate (solid line) with a calculation that sums contributions from a series of slices of the depletion zone (symbols). For the symbols, the capture rate in each slice is varied according to the fit shown in Fig. 5 and the DLTS amplitude is weighted according to the lever rule. The agreement of the capture curves obtained by these two different methods validates the use of Eq. (3) and a single capture rate for determining capture cross section.

FIG. 7. Capture cross sections of silicon defects as a function of average electric field. For the $V_2(-)$ point labeled "p-base" the electric field used in the plot is smaller than the average field because of the absence of the "dead zone" in the minority carrier inj-DLTS case. The trend lines are guides to the eye suggested by the theory of Passler (Ref. 8). The solid symbols are data reported in this paper and the open symbols are thermal cross sections taken from the literature. The thermal cross section data taken at zero applied field are plotted using a small field of 1500 V/cm to make them visible on the logarithmic scale.

ACKNOWLEDGMENTS

[1]W. Shockley and W. T. Read, Phys. Rev. **87**, 835–842 (1952).

[2]R. N. Hall, Phys. Rev. **87**, 387–387 (1952).

[3]S. M. Sze, *Physics of Semiconductor Devices*, 2nd ed. (John Wiley & Sons, New York, 1981).

[4]D. V. Lang, J. Appl. Phys. **45**, 3023–3032 (1974).

[5]G. L. Miller, D. V. Lang, and L. C. Kimerling, Annu. Rev. Mater. Sci. **7**, 377–448 (1977).

[6]P. Blood and J. W. Orton, *The Electrical Characterization of Semiconductors: Majority Carriers and Electron States* (Academic Press, 1992).

[7]C. H. Henry and D. V. Lang, Phys. Rev. B **15**, 989 (1977).

[8]R. Pässler, Solid–State Electron **27**, 155–166 (1984).

[9]A. Schenk, Solid–State Electron. **35**, 1585–1596 (1992).

[10]D. V. Lang, H. G. Grimmeiss, E. Meijer, and M. Jaros, Phys. Rev. B **22**, 3917 (1980).

[11]D. Pons, J. Appl. Phys. **55**, 3644–3657 (1984).

[12]H. Malmbekk, L. Vines, E. V. Monakhov, and B. G. Svensson, Solid State Phenom. **178–179**, 192–197 (2011).

[13]P. S. Hagan, R. W. Cox, and B. A. Wagner, in *Semiconductors*, edited by W. M. Coughran, Jr., J. Cole, P. Lloyd, and J. White (Springer, New York, 1994), Vol. 59, pp. 159–183.

[14]V. K. Arora, Appl. Phys. Lett. **80**, 3763–3765 (2002).

[15]C. Jacoboni, C. Canali, G. Ottaviani, and A. Alberigi Quaranta, Solid-State Electron. **20**, 77–89 (1977).

[16]P. M. Smith, M. Inoue, and J. Frey, Appl. Phys. Lett. **37**, 797–798 (1980).

[17]C. H. Henry, H. Kukimoto, G. L. Miller, and F. R. Merritt, Phys. Rev. B **7**, 2499 (1973).

[18]B. G. Svensson, A. Hallén, and B. U. R. Sundqvist, Mater. Sci. Eng. B **4**, 285–289 (1989).

[19]F. D. Auret and P. N. K. Deenapanray, Crit. Rev. Solid State Mater. Sci. **29**, 1–44 (2004).

[20]T. R. Oldham, *Ionizing Radiation Effects in MOS Oxides* (World Scientific, Singapore, 1999).

[21]L. Vines, E. V. Monakhov, A. Y. Kuznetsov, R. Kozlowski, P. Kaminski, and B. G. Svensson, Phys. Rev. B **78**, 085205 (2008).

[22]A. Hallén, N. Keskitalo, F. Masszi, and V. Nágl, J. Appl. Phys. **79**, 3906–3914 (1996).

[23]H. Lefèvre and M. Schulz, Appl. Phys. **12**, 45–53 (1977).

[24]S. D. Brotherton and P. Bradley, J. Appl. Phys. **53**, 5720–5732 (1982).

[25]P. Lévêque, H. K. Nielsen, P. Pellegrino, A. Hallén, B. G. Svensson, A. Y. Kuznetsov, J. Wong–Leung, C. Jagadish, and V. Privitera, J. Appl. Phys. **93**, 871–877 (2003).

[26]L. C. Kimerling, IEEE TNS **23**, 1497–1505 (1976).